DOI 10.1007/s11148-018-0194-4
Refractories and Industrial Ceramics *Vol. 59, No. 2, July, 2018*

SLAG – REFRACTORY INTERACTIONS DURING ILMENITE SMELTING: THERMODYNAMIC SIMULATION AND EXPERIMENTAL DATA

Huang Run,[1] Qian Xing,[1] Lv Xiaodong,[1] Liu Pengsheng,[1] and Zhang Jinzhu[2,3]

Translated from *Novye Ogneupory*, No. 3, pp. 28 – 33, March 2017.

Original article submitted July 24, 2017.

The interaction of four types of commonly used refractories (i.e., burned magnesite brick, magnesia carbon brick, corundum castable, and SiC castable) with slag formed in the smelting of titanium (wt. [TiO_2] = 80%) in an electric furnace at the Panzhihuan Iron and Steel plant was studied. Erosion of refractories by titanium slag was calculated using the FactSage software program. The experiment was carried out in an electric furnace based on calculation results. Meanwhile, the results of the thermodynamic simulation showed that the interaction of SiC castable with titanium slag formed TiC with a high melting point, which can prevent the slag from penetrating more deeply into the refractory and exhibits good erosion resistance. In terms of erosion resistance to titanium slag, different refractory materials can be arranged in order from most to least erosion resistant as follows: SiC castable → magnesia carbon brick → magnesite brick → corundum castable. The results of theoretical calculations are in good agreement with the experiment results.

Keywords: titanium slag, erosion, FactSage software program, thermodynamics, thermodynamic simulation.

INTRODUCTION

The 25000 kV·A electric furnace for titanium slag smelting at the Panzhihua Iron and Steel plant was developed in China in 2000 and is one of the largest in Asia. During smelting, ilmenite concentrate and a solid reducing agent (for example, anthracite coal or coke) are mixed in a certain proportion to reduce the smelt. Furthermore, iron oxide is reduced into metallic iron selectively, and titanium oxide is enriched in the slag. After the separation of slag and iron, titanium slag is obtained along with a by-product — metallic iron. The TiO_2 content in titanium slag is 75 – 85%, and since TiO_2 is an amphoteric oxide, it has a high chemical activity, reacting with almost all metals and non-metals in different environments. Therefore, it is rather difficult to choose refractory materials for lining of electric furnaces for smelting titanium slag.

Some scientists have investigated the erosion of refractories in blast furnace slag containing titanium [1 – 4] and in an electric furnace for smelting titanium slag and refractories [5 – 7]. The results showed that FeO forms fusible compounds that damage the lining of the furnace, while materials with a high melting point protect the lining from erosion. The erosion of carbon brick [8] and magnesia carbon brick [9 – 12] under the influence of titanium-free slag was also investigated, but there is little information on the erosion of the lining of electric furnaces when exposed to titanium slag. Some researchers [13, 14] studied the effect of steel slag and phosphorus-containing steel slag on the erosion of MgO–CaO material using thermodynamic phase equilibrium. Thus, it can be argued that studies of electric furnace lining erosion when exposed to titanium slag are of particular importance. The results of these studies are the key to solving the problem of increasing the service life of the furnace lining.

The authors of this article investigated the erosion of corundum castable, burnt magnesia brick, SiC castable, and magnesia carbon brick when exposed to titanium slag.

EXPERIMENTAL

The chemical composition of industrial titanium slag is as follows, wt.%: TiO_2 78.00, FeO 5.98, CaO 1.05, SiO_2 5.96, Al_2O_3 3.27, MgO 5.03. The characteristics of the investigated refractory products and concretes are presented in Ta-

[1] College of Materials and Metallurgy, Guizhou University, Guiyang, China.
[2] Guizhou Province Key Laboratory of Metallurgical Engineering and Process Energy Saving, Guiyang, China.
3 jzzhang@gzu.edu.cn

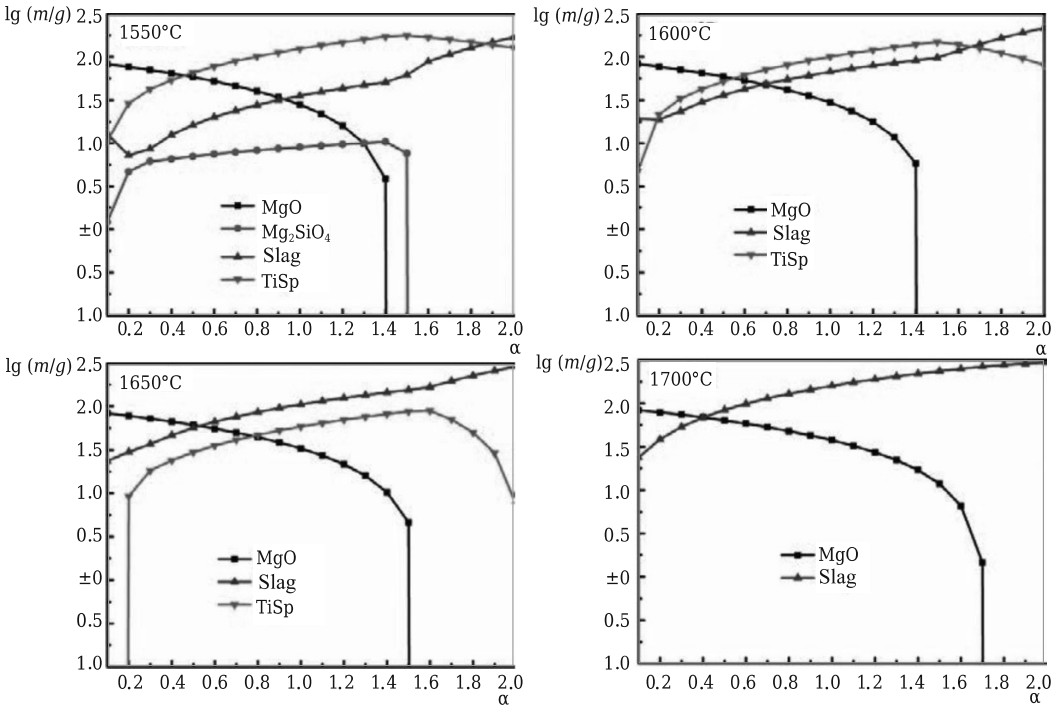

Fig. 1. Erosion of magnesite brick by titanium slag at various temperatures.

ble 1. Conditions specified in the calculations of erosion of refractory materials carried out using the FactSage software program are as follows: refractory sample mass 100 g, titanium slag sample mass with each calculation 10 g, amount of slag 0 – 200 g, temperature range 1550 – 1700 °C; α is the mass ratio of titanium slag (g) to refractory material (g), ranging from 0 to 2.

RESULTS AND DISCUSSION

Burned magnesite brick

Fig. 1 shows the erosion of burned magnesite brick by titanium slag at various temperatures. At 1550 °C, the magnesite brick reaches equilibrium after a high-temperature reaction, the main phases are MgO, forsterite (Mg_2SiO_4), slag and titanium spinel $(Mg, Fe, Al, Ti)_3O_4$ (TiSp). The amount of MgO gradually decreases as the slag content increases, and also with increasing mass ratio of MgO, forsterite, slag and TiSp. In addition, different ratios between slag and magnesite brick of variable quality yield different results: MgO is completely dissolved for $\alpha > 1.4$, forsterite — for $\alpha > 1.5$, magnesium olivine – for $\alpha > 1.7$. The forsterite phase disappears completely at 1600 °C. With gradually increasing α, the content of TiSp and slag also gradually increases. At $\alpha = 2.0$, the system still exists as slag and TiSp. For $\alpha > 1.6$, the amount of TiSp phase is small, and when the temperature reaches 1700 °C, only slag and MgO remain in the system. Finally, for $\alpha > 1.7$, only slag is present in the system, and magnesite brick is completely dissolved.

Magnesia carbon brick

Figure 2 shows the erosion of magnesia carbon brick by titanium slag at various temperatures. At 1550 °C, titanium

TABLE 1. Physicochemical characteristics of the investigated refractory aggregates.

Characteristic	Corundum castable	Burned magnesite brick	SiC castable	Magnesia carbon brick
Chemical composition, wt.%:				
Al_2O_3	91.31	1.16	8.63	—
Fe_2O_3	0.18	1.97	1.36	—
MgO	6.28	91.86	—	78.26
SiC	—	—	74.26	—
C	—	—	—	15.45
Ultimate strength, MPa:				
compressive	26.8	45.7	58.7	42.8
flexural	5.8	10.4	14.5	12.6
Load softening temperature $t_{0.6}$, °C	>1600	1550	>1600	—
Bulk density, g/cm^3	2.93	2.92	2.84	2.96
Porosity, %	15	18	16	3.8
Linear shrinkage (1500°C, 3 h), %	0.2	0.02	0.4	—
Refractoriness, °C	>1790	>1790	—	—

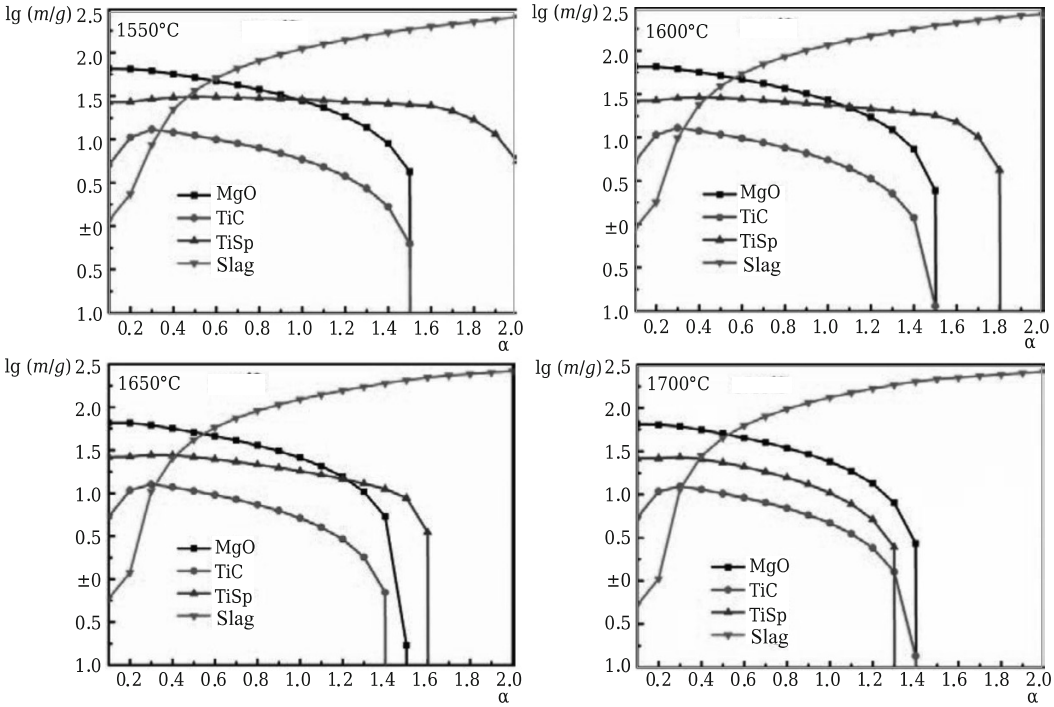

Fig. 2. Erosion of the magnesia carbon brick by titanium slag at various temperatures.

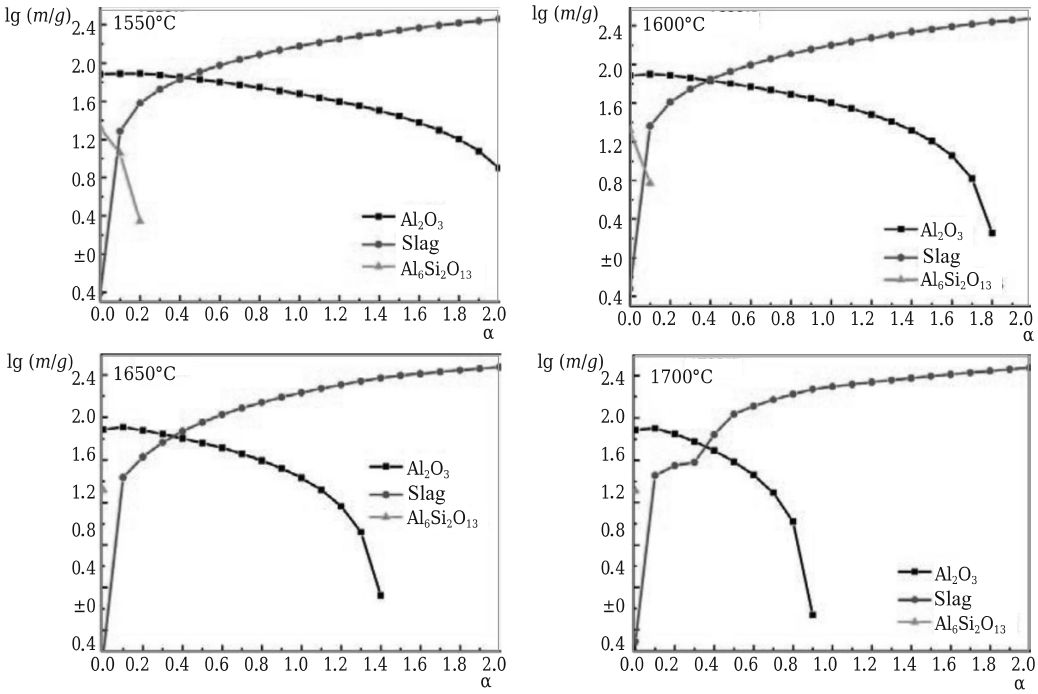

Fig. 3. Erosion of corundum castable by titanium slag at various temperatures.

slag and magnesia carbon brick achieve equilibrium, and the main phases are MgO, TiC, slag and TiSp. With increasing α, the content of MgO and TiC gradually decreases, and the content of TiSp increases at first and then decreases. MgO dissolves completely at $\alpha > 1.4$, and TiC completely disappears at $\alpha > 1.7$. As α continues to increase, the content of slag increases. At 1550°C, the mass ratio α of slag and magnesia carbon brick exceeds 1.5. As a consequence, MgO and TiC disappear. At $\alpha = 2.0$ the system continues to exist in the form of TiSp and slag. At 1600°C and $\alpha > 1.8$, only the slag

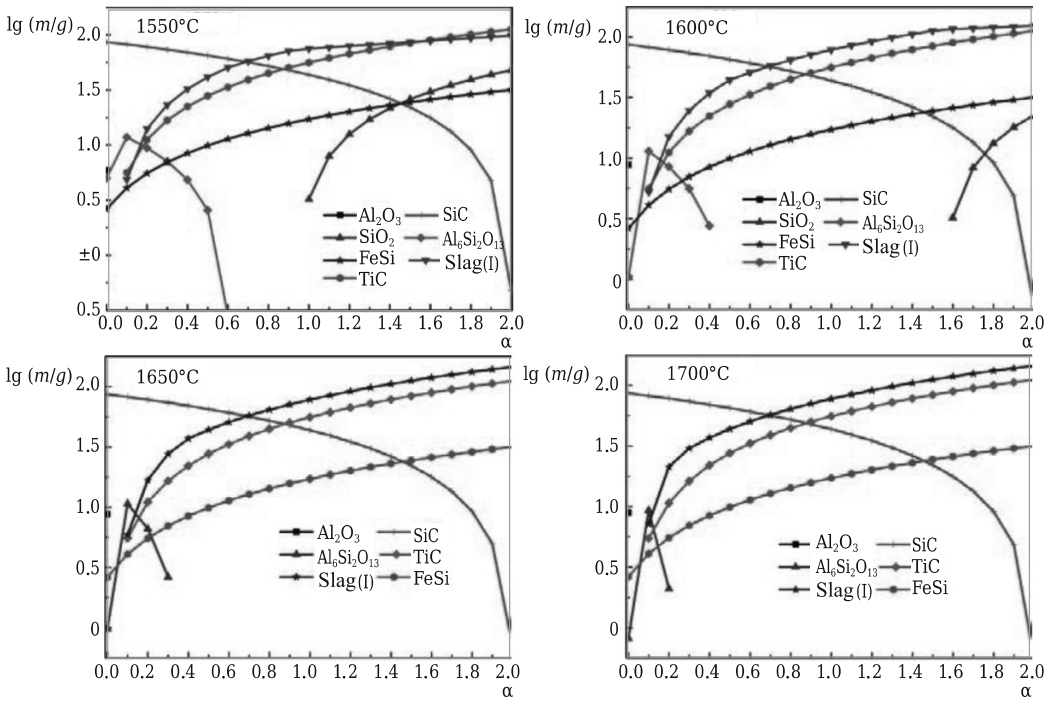

Fig. 4. Erosion of SiC castable by titanium slag at various temperatures.

phase remains in the system, and all other phases are exposed to erosion and dissolve. With increasing temperature, this trend becomes more and more obvious. At 1700°C and $\alpha > 1.4$, only the slag phase remains in the system, and magnesia carbon brick dissolves. According to the results of thermodynamic simulation, the magnesia carbon brick is eventually eroded away by titanium slag.

Corundum castable

Fig. 3 shows the erosion of corundum castable by titanium slag at various temperatures. At 1550°C, corundum castable reaches equilibrium after a high-temperature reaction with titanium slag, the main phases are Al_2O_3, $Al_6Si_2O_{13}$ and slag. As the mass ratio α of slag and corundum castable increases, the content of Al_2O_3 and $Al_6Si_2O_{13}$ gradually decreases, and the content of slag increases. $Al_6Si_2O_{13}$ completely dissolves at $\alpha > 0.3$. At 1600°C, the mass ratio becomes higher than 0.1, and $Al_6Si_2O_{13}$ completely dissolves. At $\alpha > 1.8$, Al_2O_3 completely dissolves. Furthermore, above 1650°C and after the addition of titanium slag, only the slag phase and Al_2O_3 remain in the system. As the mass ratio α increases, corundum castable undergoes rapid erosion.

SiC castable

Fig. 4 shows the erosion of SiC castable by titanium slag at various temperatures. At 1550°C, the SiC castable achieves equilibrium after a high-temperature reaction with titanium slag. The main phase consists of Al_2O_3, $Al_6Si_2O_{13}$, SiC, SiO_2, TiC, FeSi and slag. With increasing mass ratio α of slag and SiC castable, the content of $Al_6Si_2O_{13}$ and SiC gradually decreases, while the content of other components gradually increases. Given that SiC reduces titanium slag and forms SiO_2, its content increases with increasing content of titanium slag. When the mass ratio of titanium slag and SiC castable reaches 0.7, $Al_6Si_2O_{13}$ completely dissolves; the dissolution rate of $Al_6Si_2O_{13}$ increases with increasing temperature. At 1650°C, SiO_2 completely dissolves, and the content of TiC, FeSi and slag, on the contrary, gradually increases, especially with an increase in the amount of titanium slag. At 1700°C and $\alpha = 2.0$, TiC, FeSi and slag remain in the system. This indicates that the material that is formed during the erosion of SiC castable when exposed to titanium slag has a high melting point and plays a role in erosion resistance of the lining.

Experiment results

A control sample of high-Ti slag was pulverized (<0.088 mm). Two types of slag were separately stored, and the amount of moisture in them was determined. The castable refractory casting was dried. Concrete and refractory products were cut into cubes with a 60 mm edge. Grooves 28 mm in diameter and about 30 mm deep were drilled in the center of the cubes. Samples were dried for 24 hours at 110°C. Slag resistance was determined by the static crucible method. 30 g of refractory was placed in the groove containing titanium slag. The slag sample was placed in a high-temperature furnace and quickly heated to the test temperature for 3 hours. The furnace was then turned off and the sample was removed from it after cooling. After cutting the sample at the center, the width of the eroded area was measured and the erosion rate was calculated from the for-

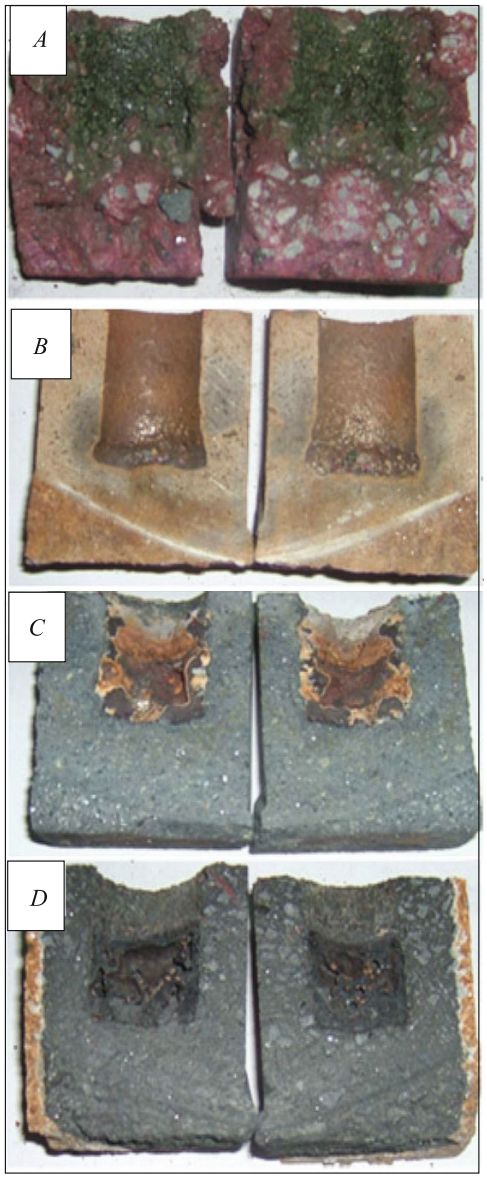

Fig. 5. Erosion profile of refractory material exposed to titanium slag: *A*) corundum castable; *B*) burned magnesite brick; *C*) SiC castable; *D*) magnesia carbon brick.

mula $(D_2 - D_1)/T$, where D_1 is the initial diameter of the slag hole, mm; D_2 is the maximum diameter of the slag hole after erosion, mm; T is the test slag resistance time, h.

The general titanium slag temperature of 1700°C was selected as the control temperature. Titanium slag was placed in a sample of corundum castable, SiC castable, magnesite and magnesia carbon brick. Samples were then placed in an electric furnace for 3 h, the temperature in the furnace was 1700°C. After cooling, the samples were taken out of the furnace and inspected for erosion. The erosion of the refractory material is shown in Fig. 5 and is described in Table 2.

It can be seen that at 1700°C, SiC castable and magnesia carbon brick exhibit the greatest slag resistance, and for SiC castable it is higher than that of the magnesia carbon brick.

TABLE 2. Description of the Erosion Profile of Refractory Samples.

Sample	Profile description and erosion	Rate of erosion, $mm \cdot h^{-1}$
Corundum castable	Loose structure, reduced strength. Slag penetrated into the sample destruction zone	—
Burned magnesite brick	Dense structure. Slag penetrated into the sample and fused with it	1.46
SiC castable	Dense structure. Good slag resistance. Clear slag line	0.60
Magnesia carbon brick	Dense structure. Decarburized layer present on the surface. Clear slag line	1.33

Thus, it can be argued that SiC castables have the greatest slag resistance and the lowest erosion rate.

CONCLUSION

Using the FactSage software program, resistance of various refractories to erosion due to exposure to titanium slag obtained from electric furnaces was calculated for various temperatures and amounts of slag. In terms of slag resistance, the investigated refractories can be arranged in the following order, from most to least erosion resistant: SiC castable → magnesia carbon brick → burned magnesite brick → corundum castable. Theoretical calculations are in good agreement with the experimental results.

The authors express their special gratitude to the National Natural Science Foundation of China (Grant No. 51404080), the Science and Technology Fund of Guizhou Province, China (Guizhou Grant J Word No. [2014] 2073) and the Doctoral Program of Guizhou University (University of Guizhou J Word No. [2013] 37).

REFERENCES

1. H. G. Du, G. T. Xu, and R. S. Diao, "Microstructure analysis of iron corrosion lining of titanium bearing blast furnace slag," *Iron Steel Vanadium Titanium*, **6**(2) (2002).
2. H. G. Du, et al., "Study on erosion of blast furnace slag by blast furnace slag," *Iron Steel*, **4**(1), 56 – 59 (2003).
3. J. Li, "Study on the mechanism of slag corrosion and improvement of material properties of blast furnace in Panzhihua Iron & Steel Co." (2002).
4. Q.-C. Liu, et al., "Corrosion resistance of MgO – C refractory to smelting reduction slag containing titania," *British Corrosion Journal*, **37**(3), 231 – 234 (2002).
5. J. Qin, et al., "Melting reduction furnace lining erosion cause analysis and improvement measures," *Refractory Material*, **4**, No. 2, 152 – 154 (2013).

6. A. M. Garbers-Craig and P. C. Pistorius, "Slag-refractory interactions during the smelting of ilmenite," *South African Journal of Science*, **102**(11/12), 575 – 581 (2006).
7. S. B. Sang, et al., "Discussion on the furnace lining material of high titanium pellet melting furnace," *Silicate Bulletin*, **6**(4) (2014).
8. Y. Chen, G. A. Brooks, and S. A. Nightingale, "Slag line dissolution of MgO refractory," *Canadian Metallurgical Quarterly*, **8**(3), 323 – 330 (2005).
9. W. Hu, et al., "Different matrix combined with the research on corrosion resistance of MgO–C brick for slag," *Silicate Bulletin*, **6**(1) (2011).
10. X. L. Fan, et al., "Slag resistance of MgO–C brick with different carbon content," *Journal of Wuhan University of Science and Technology*, **5**(4), 394 – 398 (2009).
11. H. C. Li, et al., "Effect of electromagnetic field on corrosion resistance of MgO–C refractories," *Journal of Silicate*, **6**(3), 452 – 457 (2011).
12. V. Muñoz, S. Camelli, and A. G. T. Martinez, "Slag corrosion of alumina-magnesiacarbon refractory bricks: experimental data and thermodynamic simulation," *Ceram. Int.*, **43**(5), 4562 – 4569 (2017).
13. Z. Y. Chen, "Analysis of the corrosion of MgO–CaO materials by the phase diagram," *J. Metals*, **8**(2), 62 – 69 (1983).
14. J. Berjonneau, P. Prigent, and J. Poirier, "The development of a thermodynamic model for Al_2O_3–MgO refractory castable corrosion by secondary metallurgy steel ladle slags," *Ceram. Int.*, **35**(2), 623 – 635 (2009).